Quantum transition-state theory below the crossover temperature

Dmitrii E. Makarov and Maria Topaler
School of Chemical Sciences, University of Illinois, 505 South Mathews Avenue, Urbana, Illinois 61801
(Received 17 November 1994; revised manuscript received 6 April 1995)

The quantum transition theory based on the quantum averaged effective potential is derived from first principles and critically examined in the regime where tunneling prevails over thermally activated transitions. A semiclassical approximation to the effective potential is derived, showing the relation of the present theory to the semiclassical periodic orbit approximation. We demonstrate that the centroid of a thermal path provides a proper choice of the unstable mode in transition-state theory only if the potential is symmetric or weakly asymmetric or if temperature is high enough. For a metastable potential that is not bounded from below and decreases not too slowly, the centroid density diverges, leading to infinite values of the rate; this problem can be partly cured by modifying the potential far from the transition state.

PACS number(s): 05.30.−d, 82.20.Db, 73.40.Gk, 31.70.Hq

I. INTRODUCTION

In classical transition-state theory (TST) the rate constant for surmounting a barrier is expressed in terms of equilibrium statistical mechanics

$$k=\tfrac{1}{2}uZ_0^{-1}Z^{\dagger}(x^{\dagger}), \tag{1}$$

where $u=(2k_BT/m\pi)^{1/2}$ is the average classical velocity of the particle of mass m at temperature T. Here Z_0 is the partition function of the initial state (reactants) that is calculated under the assumption that transitions over the barrier are neglected and $Z^{\dagger}(x^{\dagger})$ is the partition function of the particle that is forced to be at the transition state $x^{\dagger}$, which—in the least sophisticated version of the theory—coincides with the barrier top or the saddle point.

The centroid method [1,2] is considered the most promising candidate for a quantum transition-state theory. Its prescription is simple: Calculate the partition function of the quantum particle provided that the center of mass or *centroid* of its thermal path

$$x_0=\beta^{-1}\int_0^{\beta}d\tau\, x(\tau) \tag{2}$$

is fixed at the transition state. (Here $\beta=1/k_BT$. We will be using the system of units in which $\hbar=1$, $k_B=1$, and $m=1$ throughout the paper.) Then call this partition function $Z^{\dagger}$ and use it in Eq. (1).

Inspired by this intuitively appealing idea, several workers have applied it to assess quantum effects on various chemical reactions [3–8]. Some of these results have recently been reviewed by Voth [8]. Mills and Jonsson [7] impressively demonstrated usefulness of the so-called reversible work version of the theory (see also [9–11]). In their paper they calculated the sticking probability and free-energy barrier for dissociation of H_2 molecules on Cu(110) surface, a problem that involves six quantum degrees of freedom and many more classical dimensions. We are not aware of any other simulation method that would be applicable to a problem of such high dimensionality.

The belief that the center of mass of the thermal path x_0 should be used instead of the classical coordinate of the particle is based on Feynman's argument [12]: Consider the path-integral representation for the partition function

$$Z=\exp(-\beta F)$$
$$=\int_{x(0)=x(\beta)}D[x(\tau)]\exp\left[-\int_0^{\beta}d\tau\,H(x,\dot{x})\right], \tag{3}$$

where the classical Hamiltonian is given by $H(x,\dot{x})=\dot{x}^2/2+V(x)$. Expanding the β-periodic thermal path in a Fourier series $x(\tau)=\sum_{n=-\infty}^{\infty}x_n\exp(i\nu_n\tau)$, it is easy to see that the kinetic-energy contributions to the exponential from the Fourier components with Matsubara's frequencies $\nu_n=2\pi n/\beta$ are proportional to ν_n^2. Thus the integrand in Eq. (3) is suppressed for the paths that have Fourier components with large n. The zero Fourier component x_0 is analogous to the classical position of the particle, since integration over x_0 does not involve kinetic energy terms and reminds in this respect of integration over the classical coordinate when calculating the classical limit of the partition function.

Such an argument, of course, does not justify use of x_0 as a replacement for the classical position at low temperatures, especially the $T=0$ limit, where Matsubara's frequencies are vanishingly small and contributions from all Fourier components are significant. Gillan, however, demonstrated [1] that the centroid formula reproduces the correct golden rule rate for a double well coupled to a bath of classical oscillators, provided the classical velocity is replaced by a different velocity factor

$$u=(8\pi)^{1/2}\Delta x/\beta, \tag{4}$$

where Δx is the width of the centroid distribution, which is assumed to be Gaussian. Even though the bath is considered classical, this is the deep tunneling regime for the double well. This is still not completely convincing: the

double well Gillan considered was symmetric. For such a potential the centroid constraint is not too restrictive because any "typical" path (e.g., a semiclassical tunneling trajectory) should have its centroid situated at the barrier top.

Later, Voth, Chandler, and Miller [2] justified the centroid theory as a generalization of classical transition-state theory and explained the way dynamical corrections to the centroid formula can be calculated. They also justified use of centroids below the crossover temperature using semiclassical periodic orbit (instanton) theory and derived the velocity factor in Gillan's form Eq. (4), assuming that the centroid-constrained partition function is Gaussian near the transition state.

Amusingly, the origin of the width Δx is quite different in the cases of Gillan and of Voth, Chandler, and Miller. In Gillan's model, Δx results from coupling of the reaction coordinate to a bath of classical oscillators. In Voth, Chandler, and Miller's case Δx is an intrinsic property of the one-dimensional model they considered. Apparently, there should be a more universal and less model-dependent derivation of the velocity factor Eq. (4).

Given the fact that the centroid method has proven to be a very useful methodology for computing quantum-mechanical rates in many-body systems, understanding its strengths and limitations is very important. Do we obtain a better theory than other existing approximations by using centroids at low temperature? The main advantage of the centroid approach as compared to others seems to be that quantum-mechanical partition functions are routinely evaluated numerically using imaginary-time path integrals, so one is not restricted to the stationary phase approximation to the path integral, as in the case of semiclassical theories, or to the spin-boson Hamiltonian approximation to the tunneling system, with small tunneling amplitude, as in golden-rule-type theories. The existing derivations of the centroid relations and of the velocity factor Eq. (4) in the low-temperature case, though, start from the above two approximations. The only notable exception is an insightful article by Stuchebrukhov [13], which clarifies some of the questions posed above. Stuchebrukhov shows in his paper that for some potentials the Gaussian approximation breaks down for a certain finite temperature and Δx formally becomes infinite. Moreover, the centroid density may have a minimum, either local or global, rather than a maximum at the barrier top.

Still, use of centroids appears as a very tempting alternative to other statistical mechanical rate theories. "Exact" methods based on the flux-flux correlation function formalism can be implemented only for low-dimensional problems, although effects of coupling to a multidimensional dissipative reservoir can be incorporated exactly [14]. Semiclassical instanton-type theories turned out to be very successful in two or three dimensions [15–18]; however, the problem of finding periodic orbits in higher dimensions may become severe. Also the stationary phase approximation inherent to instanton theories may not be sufficient to describe strongly anharmonic potentials. The centroid formulation is not plagued by any of these difficulties.

Rigorously formulating and testing the centroid theory below the crossover temperature where tunneling prevails over thermal transitions are the goals of this paper. In Sec. II we derive the centroid result from the ImF formulation of rate theory. We show that the centroid coordinate is a convenient (but not unique) choice of the unstable mode that is to be continued to the complex plane in order to regularize the partition function of a metastable state and obtain its imaginary part. In Sec. III we describe a semiclassical theory for the effective potential. This theory offers an alternative to various variational approximations to the effective potential [2,13,19] and, being a rigorous steepest-descent limit of the path integral for the centroid density, provides deeper insight into the relation between the semiclassical bounce (periodic orbit) theory and centroid formulation and explains how strong quantum fluctuations described semiclassically as bounce trajectories give rise to the lowering of the effective potential as compared to the classical one. In Sec. IV we attempt to apply the formulated theory to a cubic parabola potential and discover that it does not work because the centroid constraint fails to eliminate the divergence of the partition function. We argue that the problem we encounter is generic when the decay rate of a metastable unbound potential is calculated. In order to avoid the divergence problem, we modify the potential by setting it to a constant value far to the right of the barrier and eventually test our theory against the exact solution. We find that the centroid approximation works only if the modified potential is not too asymmetric. In order to better understand when and why the centroid method fails, a toy model is described in the Appendix that mimics the properties of the action as a function of Fourier components of the thermal path. Finally, Sec. V concludes by discussing the nature of the approximations involved in the centroid theory and outlines a quantum transition-state theory free of those limitations.

II. DERIVATION OF CENTROID RELATIONS FROM THE ImF METHOD

Consider a particle tunneling out of a metastable potential described, e.g., by a cubic parabola $V(x)=\omega_0^2 x^2(1-x/l)/2$. The minimum of this potential is at $x=0$, the maximum at $x=x^*$. The decay rate of an isolated "eigenstate" with complex energy $E_n=E_n^0-i\Gamma_n/2$ is given by $-2\,\mathrm{Im}E_n=\Gamma_n$, where we assume that $\Gamma_n \ll \omega_0$. The overall tunneling rate is then given by Γ_n averaged over the Boltzmann distribution among the energy levels E_n^0:

$$k=Z_0^{-1}\sum_n \Gamma_n e^{-\beta E_n^0} \approx 2\beta^{-1}\,\mathrm{Im}Z/Z_0 = 2\,\mathrm{Im}F\ , \qquad (5)$$

where $Z_0=\sum_n \exp(-\beta E_n^0)$ is the partition function of reactants and F is the free energy of the system.

Before we proceed, two remarks are in order. First, based on an underlying assumption of transition-state theory, Eq. (5) does not take into account the possibility of nonequilibrium population among the energy levels, i.e., the energy diffusion regime [20]. Strictly speaking,

this is possible only if the reaction coordinate is coupled to a continuum of environmental degrees of freedom. At high temperatures the coupling, which classically appears as a friction force [20], should be strong enough that the energy levels lying near the barrier top are not depleted. In the deep tunneling regime where the transition occurs from lower-lying energy levels, much weaker coupling is required in order to maintain the Boltzmann distribution [14,20].

The second comment concerns the applicability of Eq. (5) to the case where the potential is not metastable but consists of two wells ("reactant" and "product" valleys) separated by a barrier. We can still consider the reactant well as a metastable state as if the particle disappears once it has crossed the barrier. Equation (5) in this case will yield the forward rate of transitions from reactants to products. Similar consideration of the product state will give the backward rate constant. This is true, though, if there is no phase coherence between the reactant and product states; otherwise the rate constant may either not be defined or be affected by coherence [14]. Weiss *et al.* [22] justified use of the ImF method for the case of dissipative tunneling in a slightly asymmetric double well and showed that this method gives the same result as real-time calculations as long as tunneling is incoherent and the rate constant can be defined.

In principle, the free energy F given by Eq. (3) diverges for an unbound Hamiltonian. In the complex scaling method, the coordinate is allowed to be complex in order to find complex resonances by solving a Schrödinger equation [21,23]. Similarly, thermal paths in the path integral of Eq. (3) should be allowed to be complex valued, in order to regularize the path integral and to find the imaginary part of the free energy; no general numerical procedure is available that does so. That is why Eq. (5) is not suited for computation. In semiclassical bounce (instanton) theories (see, e.g., [16,17,24]), Eq. (5) is evaluated using the steepest-descent approximation [25]. The stationary points of the action

$$S=\int_0^\beta d\tau\, H(x,\dot{x}) \tag{6}$$

are classical β-periodic trajectories in the upside-down potential. Two trivial trajectories $x\equiv 0$ and x^* correspond, respectively, to the reactant partition function Z_0 and to thermally activated transitions over the barrier. The bounce solution exists below the crossover temperature

$$T_c=1/\beta_c=\omega^*/2\pi\ , \tag{7}$$

where ω^* is the unstable frequency of the barrier. This solution represents neither a minimum nor a maximum of the action but a saddle point in the space of thermal paths. The path integral Eq. (3) diverges along the direction of the unstable mode in the function space; however, it can be regularized by continuing integration into the complex plane. It is important that integration along all other modes except one is well defined and does not require any analytical continuation. In other words, stationary point analysis of the path integral Eq. (3) provides a natural way to define a single unstable mode and then to regularize the integral along this mode using the steepest-descent approximation.

In general, the choice of the unstable mode is by no means unique, as long as it provides the necessary regularization of Eq. (3). We show below that the zero Fourier component of the path, that is, its center of mass, provides another, more convenient from a numerical viewpoint, choice of the unstable coordinate.

By introducing the effective potential $V_{\rm eff}$ or, equivalently, the centroid density

$$\begin{aligned}\rho(x_c)&=\exp[-\beta V_{\rm eff}(x_c)]\\&=(2\pi\beta)^{1/2}\int D[x(\tau)]\delta(x_c-x_0)\\&\quad\times\exp\left[-\int_0^\beta d\tau\, H(x,\dot{x})\right]\ ,\end{aligned} \tag{8}$$

the partition function Eq. (3) is recast in a classical form

$$Z=(2\pi\beta)^{-1/2}\int dx_c\,\exp[-\beta V_{\rm eff}(x_c)]\ . \tag{9}$$

Thus far no approximation has been made. Below, the integral (9) is evaluated by the method of steepest descent.

Assume that the effective potential has one minimum at $x_c=x_r$ and a maximum at $x_c=x^\dagger$. Generally, we do not necessarily expect $V_{\rm eff}(x_c)$ to have qualitatively the same shape as the original potential $V(x)$, e.g., it may have several local maxima and minima; the treatment below can be straightforwardly extended to the case of multiple stationary points if the maxima and the minima of the effective potential are well separated. Obviously, unless $V(x)$ is symmetric, $x^\dagger$ does not coincide with the maximum of $V(x)$. The integrand in (9) has two stationary points $x_c=x_r,x^\dagger$. Following Affleck's procedure for the classical case [26], the point $x_c=x_r$ is a stable point; integration in the vicinity of this point gives the partition function of reactants Z_0. To evaluate the contribution from the second fixed point we expand the potential $V_{\rm eff}$ in a series around this point to obtain

$$\begin{aligned}&\exp[-\beta V_{\rm eff}(x)]\\&\quad=\exp[-\beta V_{\rm eff}(x^\dagger)]\exp[\tfrac{1}{2}\beta|V''_{\rm eff}(x^\dagger)|(x-x^\dagger)^2]\ ,\end{aligned} \tag{10}$$

where $V''_{\rm eff}(x^\dagger)<0$.

The integral over x is Gaussian and diverges, but after extending the integration contour into the complex plane of x and performing the integration using the method of steepest descent one obtains

$$\mathrm{Im}Z=\frac{1}{2\beta|V''_{\rm eff}(x^\dagger)|^{1/2}}\exp[-\beta V_{\rm eff}(x^\dagger)]\ . \tag{11}$$

Substituting this into (5) we obtain

$$k=\frac{1}{\beta^2 Z_0|V''_{\rm eff}(x^\dagger)|^{1/2}}\exp[-\beta V_{\rm eff}(x^\dagger)]\ . \tag{12}$$

From Eq. (10), $\rho(x_c)$ near the point $x^\dagger$ is a Gaussian distribution with width equal to

$$\Delta x^2=[\beta|V''_{\rm eff}(x^\dagger)|]^{-1}\ . \tag{13}$$

The centroid-constrained partition function at $x=x^\dagger$ is

$$Z_c(x^\dagger)=(2\pi\beta)^{-1/2}\exp[-\beta V_{\rm eff}(x^\dagger)] . \quad (14)$$

Using (13) and (14), (12) takes the form

$$k=(2\pi)^{1/2}\beta^{-1}Z_0^{-1}\Delta x Z_c(x^\dagger) , \quad (15)$$

which is Gillan's result [1] provided that $x^\dagger$ is used as the position of the transition state. Using the definition of the velocity Eq. (4), Eq. (15) can be written in the form of Eq. (1).

Note that Eq. (12) is not the classical transition-state theory rate for the potential $V_{\rm eff}(x)$. If we assume that k should be the rate of classical transitions in $V_{\rm eff}(x)$, then one should introduce Affleck's correction factor [26] ϕ such that

$$k=2\phi\,{\rm Im}F , \quad \phi=\beta|V''_{\rm eff}(x^\dagger)|^{1/2}/2\pi , \quad (16)$$

which results in a TST-like formula that is consistent with the high-temperature limit:

$$k=\frac{1}{2\pi\beta Z_0}\exp[-\beta V_{\rm eff}(x^\dagger)] . \quad (17)$$

This is the usual centroid theory result obtained in [2]. For low temperatures Eq. (12) should be valid rather than Eq. (17).

These formulas can also be easily extended to the multidimensional case: Suppose that the n-dimensional effective potential $V_{\rm eff}(\mathbf{x})$ has only one saddle point $\mathbf{x}=\mathbf{x}^\dagger$. Then introducing local normal coordinates at the saddle point that include one unstable mode s ("tunneling reaction coordinate") and a set of stable modes q_i, $i=1,\ldots,n-1$, and repeating the previous reasoning we obtain for the rate constant

$$kZ_0=(2\pi)^{n/2}\beta^{-1}\Delta s\left[\prod_{i=1}^{n-1}[\beta V_{{\rm eff},ii}(\mathbf{x}^\dagger)]^{-1/2}\right]Z_c(\mathbf{x}^\dagger) , \quad (18)$$

where the width of the centroid density distribution is measured along the unstable mode

$$\Delta s^2=[\beta|V_{{\rm eff},ss}(\mathbf{x}^\dagger)|]^{-1} . \quad (19)$$

III. SEMICLASSICAL THEORY OF EFFECTIVE POTENTIAL

Several approximations have recently been proposed for the quantum averaged effective potential Eq. (8); see, e.g., [2,8,12,13,19,27,28]. Most of these theories are based on a variational estimate for Eq. (8). Although the path integral of Eq. (8) can be evaluated numerically, those theories offer invaluable insight into the role of quantum fluctuations in enhancing the transition rate. Presented below is a semiclassical estimate for Eq. (8), which provides additional physical insight into the role of quantum fluctuations, since the interesting physics inherent to a potential that has several extrema is often masked in a variational theory by using a harmonic oscillator reference. Also the semiclassical effective potential [which can be thought of as the potential along a "minimum action path" (MAP) in the space of thermal paths, in analogy to the "minimum energy path" [17] extensively used in classical rate theory] may be a good reference for evaluating the quantum-mechanical rate in much the same way as this is done in classical TST. This idea will be further discussed in Sec. V.

A. Derivation

We start from the definition Eq. (8) for the effective potential. Replacing the δ function by a Gaussian $(2\pi)^{-1/2}\sigma^{-1}\exp(-x^2/2\sigma^2)$ gives

$$\exp[-\beta V_{\rm eff}(x_c)]=(2\pi\beta)^{1/2}\frac{1}{(2\pi)^{1/2}\sigma}\times\int D[x(\tau)]\exp\{-S_{\rm eff}[x(\tau)]\} , \quad (20)$$

where

$$S_{\rm eff}=\int_0^\beta d\tau[\tfrac{1}{2}\dot{x}^2+V(x)]-\frac{x_c}{\beta\sigma^2}\int_0^\beta d\tau\,x(\tau)+\frac{x_c^2}{2\sigma^2}+\frac{1}{2\beta^2\sigma^2}\left[\int_0^\beta d\tau\,x(\tau)\right]^2 . \quad (21)$$

Our strategy is to carry out all calculations with finite σ and take the $\sigma\to 0$ limit at the end to recover the stationary phase approximation for the original path integral Eq. (8). The stationary phase approximation in the path integral amounts to demanding

$$\delta S_{\rm eff}[x(\tau)]/\delta x(\tau)=0 ,$$

which gives the following equation of motion for the "bounce:"

$$-\frac{d^2x}{d\tau^2}+\frac{d}{dx}\left[V(x)-\frac{x_c}{\beta\sigma^2}x\right]+\frac{1}{\beta^2\sigma^2}\int_0^\beta d\tau\,x(\tau)=0 . \quad (22)$$

Using the definition of the centroid coordinate Eq. (2), the bounce equation can be rewritten as

$$-\frac{d^2x}{d\tau^2}+\frac{dV(x)}{dx}=\frac{1}{\beta\sigma^2}(x_c-x_0) . \quad (23)$$

Equations (2) and (23) should be solved self-consistently because x_0 is an undefined variable that should satisfy both of them. The bounce action is given by

$$S_b=\int_0^\beta d\tau\{\tfrac{1}{2}\dot{x}^2+V[x(\tau)]\}+\frac{1}{2\sigma^2}(x_0-x_c)^2 , \quad (24)$$

where $x(\tau)$ is the solution to Eq. (23).

The limit $\sigma\to 0$ is tricky. Since the right-hand side of Eq. (23) should not be infinite, we obtain $x_0\to x_c$. However, if the right-hand side of Eq. (23) is zero, this equation becomes the usual equation of motion in the potential $-V(x)$ and the centroid position of the trajectory x_0 cannot coincide with an arbitrary value of x_c. Therefore, x_c-x_0 should scale as σ^2 so that

$$a=(x_c-x_0)/\sigma^2 \quad (25)$$

remains constant.

To calculate the prefactor, expand the action around the stationary point

$$S_{\text{eff}}=S_b+\tfrac{1}{2}\int_0^\beta d\tau\int_0^\beta d\tau'\delta x(\tau')\frac{\delta^2 S_{\text{eff}}}{\delta x(\tau)\delta x(\tau')}\delta x(\tau)\ , \quad (26)$$

where the path is represented as $x+\delta x$, x being the bounce solution of Eq. (23). For the second derivative we obtain

$$\frac{\delta^2 S_{\text{eff}}}{\delta x(\tau)\delta x(\tau')}=\delta(\tau-\tau')\left[-\frac{d^2}{d\tau^2}+V''\right]+\frac{1}{\beta^2\sigma^2}\ . \quad (27)$$

Integration over δx can be performed by diagonalizing the second derivative operator defined as

$$\hat{L}(\sigma)y=\left[-\frac{d^2}{d\tau^2}+V''[x_b(\tau)]\right]y(\tau)+\frac{1}{\beta^2\sigma^2}\int_0^\beta d\tau\, y(\tau)\ , \quad (28)$$

$$\hat{L}(\sigma)y_n(\tau)=\varepsilon_n y_n(\tau)\ . \quad (29)$$

Representing this operator in the basis of Fourier components of δx, it is easy to see that one eigenvalue ε_0 behaves as σ^{-2} in the limit $\sigma\to 0$, which leads to cancellation of the infinite prefactor in Eq. (20). This infinite positive eigenvalue replaces the zero eigenvalue that exists in the spectrum of $\hat{L}(\infty)$ (that is, in the absence of the centroid constraint on the path integral) and is common in the bounce theory [24]. The spectrum of $\hat{L}(\sigma\to 0)$ is therefore positive and the determinant of this operator $D(\sigma)=\det\hat{L}(\sigma)$ is well defined. This determinant is a properly regularized product of ε_n's; the normalizing factor can be determined by taking the limit of free particles of harmonic oscillators (see below).

After taking the $\sigma\to 0$ limit we arrive at the following prescription for calculating V_{eff} semiclassically.

(i) Solve the equation of motion

$$-\frac{d^2x}{d\tau^2}+\frac{dV(x)}{dx}=a(x_c)/\beta \quad (30)$$

together with

$$x_c=\beta^{-1}\int_0^\beta d\tau\, x(\tau)\ , \quad (31)$$

which determines $a(x_c)$. Equation (30) is simply the bounce equation for the potential $V(x)-a(x_c)x/\beta$. Note that $a(x_c)$ can be recognized as a Lagrange multiplier that is to be introduced in order to minimize the action of Eq. (6) with an additional constraint Eq. (31).

(ii) The effective potential is then given by

$$\beta V_{\text{eff}}(x_c)=\int_0^\beta d\tau\{\tfrac{1}{2}\dot{x}^2+V[x(\tau)]\}+\tfrac{1}{2}\lim_{\sigma\to 0}\ln[\sigma^2\det\hat{L}(\sigma)/\beta]\ . \quad (32)$$

Note that normalization of the determinant $D(\sigma)$ leads to a constant shift in the effective potential and is therefore of no concern.

If it were not for the last term in Eq. (32), the standard instanton solution that obtains from Eq. (30) if $a(x_c)=0$ would provide a stationary point (typically, a maximum) of the effective potential, in accord with the result of [2]. This stationary point is somewhat shifted though, due to the prefactor.

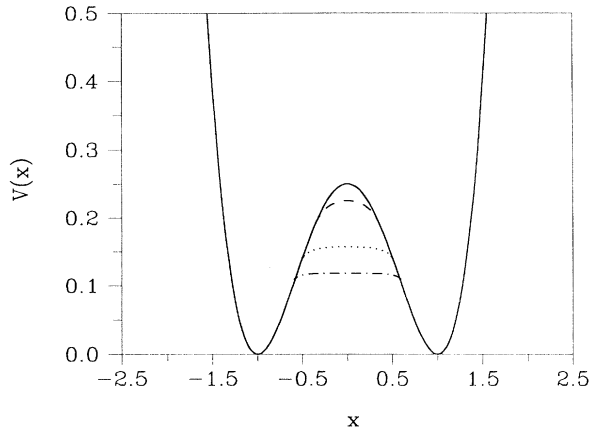

FIG. 1. Semiclassical effective potential at $\beta\omega_0=0.0$, 8.0, 12.0, and 16.0 (solid, dashed, dotted, and dash-dotted lines, respectively) for the symmetric quartic potential given by Eq. (35) with $F=0$. The energy and the coordinate are measured in dimensionless units, as described in the text.

As an illustration, one obtains a "classical" effective potential by assuming that the dominant contribution to the path integral comes from the trivial solution

$$x\equiv x_c$$

such that $a(x_c)/\beta=V'(x_c)$. The prefactor is evaluated by expanding the path in a Fourier series [19] to give

$$\exp[-\beta V_{\text{eff}}(x_c)]=\frac{\beta\omega(x_c)/2}{\sinh[\beta\omega(x_c)/2]}\exp[-\beta V(x_c)]\ , \quad (33)$$

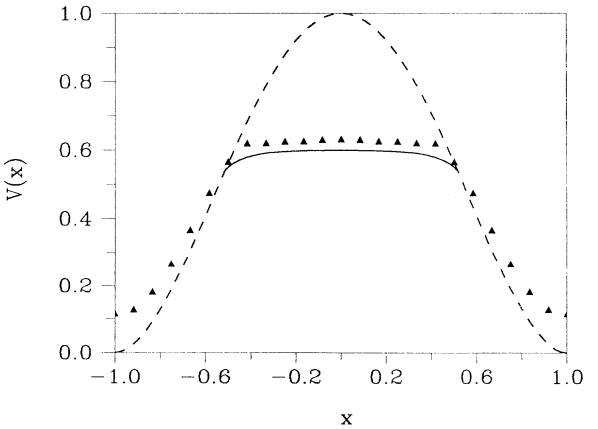

FIG. 2. Semiclassical (solid line) and exact (markers) effective potentials for the symmetric quartic potential [Eq. (35) with $F=0$] at $T=T_c/2$. $V_0/\hbar\omega_0=17.0$. The dashed line indicates the potential $V(x)$; the semiclassical effective potential is plotted only where it is different from $V(x)$.

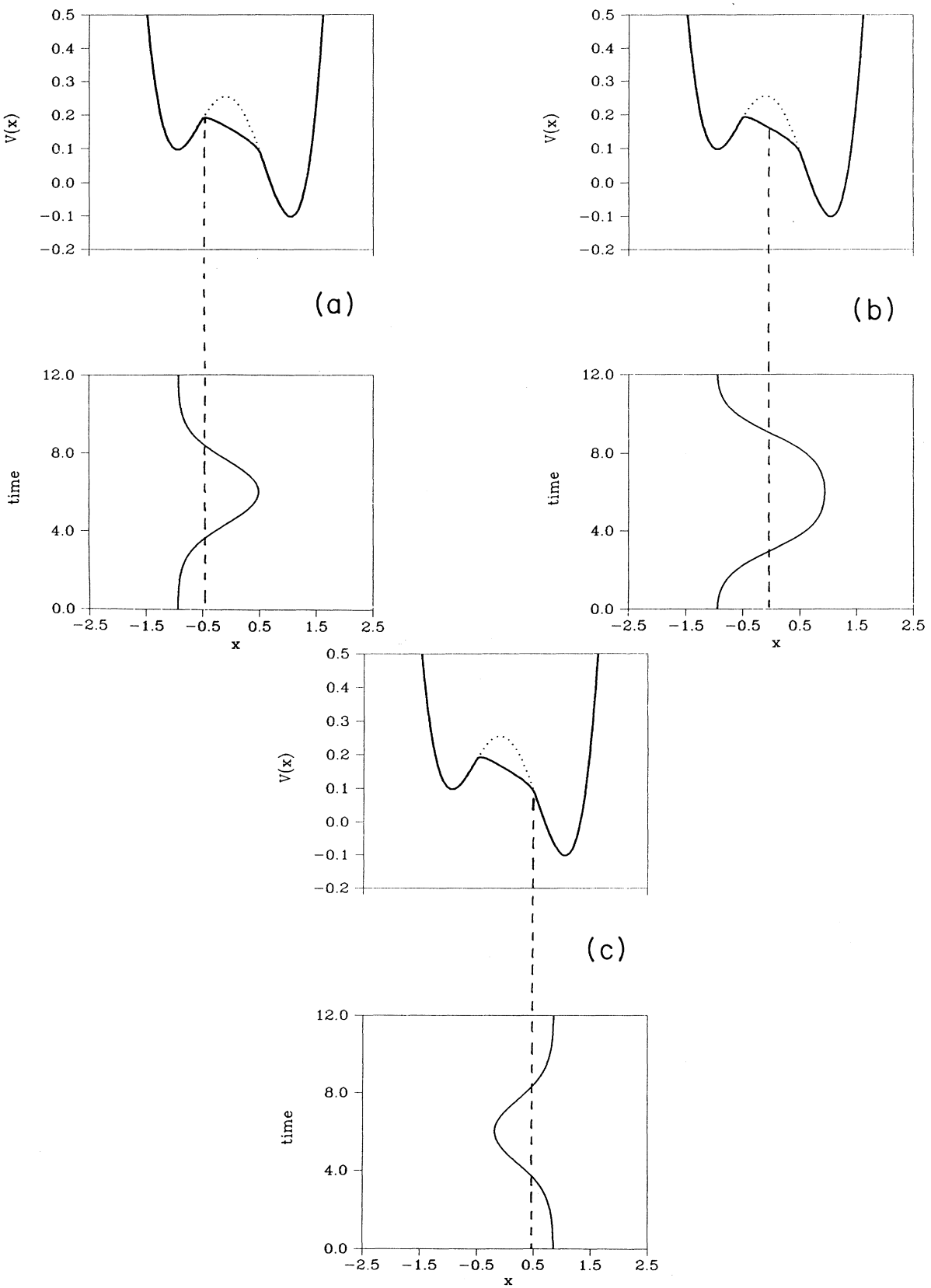

FIG. 3. Semiclassical effective potential (upper part of the figure) and the bounce solution $x(\tau)$ of Eq. (30) (lower part) for the potential of Eq. (35) with $F=0.1$. Dotted lines indicate the potential $V(x)$, solid lines the effective potential. The vertical dashed lines indicate the centroid position $x_c=-0.5$, 0, and 0.5 for (a)–(c), respectively.

where $\omega^2(x_c)=V''(x_c)$. Equation (33) is the high-temperature limit of the Feynman-Kleinert effective potential [19]. At lower temperature, they modified the frequency $\omega(x_c)$ and the potential $V(x)$ using a Gaussian smearing procedure to obtain a better reference functional for variational evaluation of the path integral. In other words, Feynman and Kleinert's procedure implies that the integration over nonzero Fourier components of the path is Gaussian, with an optimized dispersion that depends both on temperature and on the potential shape. In our semiclassical approach fluctuations around the point x_c are dominated by a large bouncelike optimum fluctuation that appears when temperature is low enough. Divergence of the classical expression Eq. (33) at the poles of the prefactor where $i\omega(x_c)\beta=2\pi$ signals the onset of these large non-Gaussian fluctuations.

B. Example: Asymmetric double well

Consider the potential

$$v(q)=V_0V(x) \tag{34}$$

where

$$V(x)=\tfrac{1}{4}(x^2-1)^2-Fx \tag{35}$$

is a dimensionless potential expressed as a function of the dimensionless coordinate $x=q/q_0$. We also measure time in dimensionless units $t'=\omega_0 t$ such that the total classical Hamiltonian becomes $H=V_0[\frac{1}{2}\dot{x}^2+V(x)]$, $V_0=\omega_0^2q_0^2$. To avoid tedious calculation of preexponential factors, consider the asymptotic semiclassical limit of $V_0/\hbar\omega_0\gg 1$; the logarithmic term in Eq. (32) can simply be neglected in this case. It is in this limit that the semiclassical approximation is expected to become exact. Of course, the rate vanishes in this limit; however, we can study the quantity $(\hbar\omega_0/V_0)\ln k$, which remains finite. The classical effective potential Eq. (33) coincides with $V(x)$ in this limit.

For $T>T_c$ no bounce solutions exist. As temperature is decreased below T_c there appears a range of x values where the bounce solution exists. The center of mass of such a bounce solution is, roughly speaking, comprised between the two points where $|\omega(x_c)|\beta=2\pi$; the region spanned by bounces increases as temperature is lowered.

This picture is illustrated in Fig. 1, where the semiclassical effective potential is plotted at different temperatures for the symmetric case ($F=0$). At very low temperatures the effective potential becomes flat, with $V''_{\rm eff}(x_c)\to 0$. The height of the effective barrier also tends to zero $V^{\dagger}_{\rm eff}\to S_b^0/\beta$, where S_b^0 is the bounce action at zero temperature (if the prefactor is taken into account, it tends to the energy of the ground state, which is small compared to V_0 in our approximation). The centroid density therefore becomes a constant value between the two potential minima, a result that is in accord with the two-state model of Gehlen and Chandler for electron transfer [29], as well as with Gillan's prediction [1]. Vanishing of the curvature of the effective potential at zero temperature does not mean that the centroid expression for the rate constant diverges: Even though $\Delta x\to\infty$, the factor $1/\beta$ in Eq. (15), together with the exponentially growing partition function of the reactants, compensates for this effect. The semiclassical effective potential is in good agreement with the exact result obtained by Monte Carlo sampling of the path integral of Eq. (8), as shown in Fig. 2.

In Figs. 3(a)–3(c) the effective potential is shown for an asymmetric case $F=0.1$, $\beta\omega_0=12.0$. The dashed line indicates the classical potential. Bounces exist in the region where the dashed line is different from the solid line, which represents the semiclassical approximation for the effective potential. In the lower part of each figure the bounce solutions $x(\tau)$ that satisfy Eq. (30) and provide the dominant contribution to the effective potential at points $x_c\approx -0.5$, 0.0, and 0.5 are shown. This bounce has a large amplitude and spans a large part of the barrier; for $x_c\approx 0.0$ the bounce solution spans the whole barrier, i.e., even though the area occupied by bounces is not too wide yet at this temperature, the effective potential is determined by the global shape of the barrier.

IV. DECAY OF METASTABLE STATE

The centroid theory is known to provide accurate results for transmission through a symmetric Eckart barrier [2]. In this section the centroid theory is tested for a metastable potential. The cubic parabola potential

$$V(x)=\tfrac{1}{2}\omega_0^2x^2(1-x/l) \tag{36}$$

is a prototypical model in tunneling studies [24,23]. Benchmark calculations of resonance positions and widths by the complex scaling method have been reported by Hontscha, Hänggi, and Pollak [23]. In this section we wish to find out whether the result given by the centroid formula (12) will agree with the exact rate constant obtained in [23]. However, substituting Eq. (36) into Eq. (8) one finds that the resulting centroid-constrained partition function diverges. Formally, this can be seen by representing the path integral of Eq. (8) as an integral over Fourier components of the path $x(\tau)$. The source of divergence is not only the integration over the zero Fourier component x_0, which is eliminated by the centroid constraint $x_c=x_0$, but integration over all other Fourier components as well. Indeed, cubic terms in the exponential in addition to the quadratic terms necessarily lead to a divergent integral.

The divergence of the centroid-constrained partition function can be understood as follows: Suppose the centroid of the thermal path is fixed at $x_0=x_c$. Normally, large deviations of $x(\tau)$ from x_c are prohibited by large kinetic-energy contribution to the action they entail. For example, if the thermal path reaches a remote point at some moment τ_1, $x(\tau_1)\gg l$, then the kinetic-energy contribution to the action will be on the order of $[x(\tau_1)-x_c]^2/2\beta$. However, the potential-energy contribution approximately equal to $\beta V[x(\tau_1)]$, will favor such a large fluctuation if the potential $V(x)$ is unbounded from below and goes to $-\infty$ faster than $-x^2$ as $x\to\infty$. Therefore, the integrand of Eq. (8) can be made arbitrari-

ly large and the integral diverges.

Such a reasoning does not exclude the possibility of a local minimum of the integrand. In fact, the classical effective potential Eq. (33), which is obtained with the assumption that the thermal path does not deviate too much from the static solution $x \equiv x_c$, corresponds to such a minimum. Beyond the Gaussian approximation Eq. (26) we will discover that a large enough fluctuation δx can make the integrand arbitrarily large. Therefore, for $\beta > 0$ the static solution provides a local but not the global minimum of the integrand in Eq. (8). (This minimum becomes global if the inverse temperature β is exactly zero.) For the potential of Eq. (36) one also finds nontrivial bounce solutions whose centroids are located to the left of the barrier; the action for such a bounce is greater than that of the static solution. These bounces correspond to local maxima of the action. The existence of such local extrema of the action explains the following paradox: In a way different from ours the authors of [2] showed that the semiclassical result for the rate can be recast in the form of Eq. (15). Instead of a naturally expected improvement, one may run into serious trouble trying to use the exact value of $\rho(x)$ instead of its semiclassical counterpart. Indeed, for a metastable potential $\rho(x)$ diverges. Moreover, for $T \gg T_c$ the classical effective potential of Sec. III A gives the correct value of the rate constant (see, e.g., [2,20]), while the true centroid density Eq. (8) diverges for arbitrarily high (but finite) temperature. This paradox is further discussed in the Appendix.

We find therefore that the centroid constraint eliminates the divergence of the partition function, as claimed in Sec. II, only if the potential is either bounded from below or decreases slowly enough. In practice, this is not a very stringent condition: Most of the potentials that are relevant for rate theory are bounded from below and use of potentials such as Eq. (36) is an idealization. If the potential (36) is modified to be constant $V(x) \equiv V(x_m) \equiv V_m$ for $x \geq x_m > l$, then the rate should not be very sensitive to the choice of x_m. For example, using the semiclassical theory, the rate constant is *precisely the same* for any choice of x_m because the bounce solution obviously never reaches the point x_m. Furthermore, it has been shown in [23] that for $V^*/\hbar\omega_0 = 2m\omega_0 l^2/27\hbar = 3$ the instanton estimate of the rate constant at $T \ll T_c$ agrees with the exact result within 10%.

These observations suggest the above modification of the potential as a good way to cure the divergence problem. We evaluated the effective potential needed in Eq. (12) by the Monte Carlo sampling of the path integral Eq. (8) in the Fourier representation. The results are presented in Fig. 4, where an Arrhenius plot of the rate constant $[\log_{10}(k/\omega_0)$ vs $T_c/T]$ obtained using Eq. (12) is shown for two values of V_m, together with the exact numerical data for the cubic parabola potential [23]. For energy $V_m = -V^*/3$ that is not very low and comparable with the zero-point energy, the centroid result for the modified potential follows closely the exact result for the cubic parabola down to the temperatures where the low-temperature plateau of the rate is reached. However, for

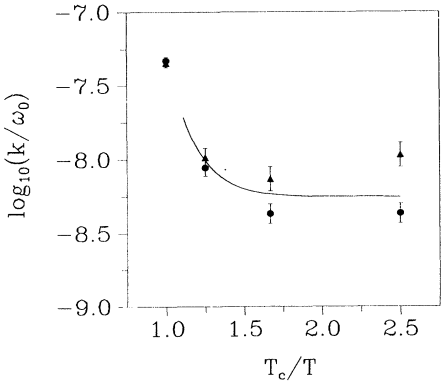

FIG. 4. Arrhenius plot of the rate constant for the modified cubic parabola potential of Sec. IV obtained by using Eq. (12). Solid line, complex scaling data from [23]; circles, $V_m = -V^*/3$; triangles, $V_m = -V^*$. $V^*/\hbar\omega_0 = 3.0$.

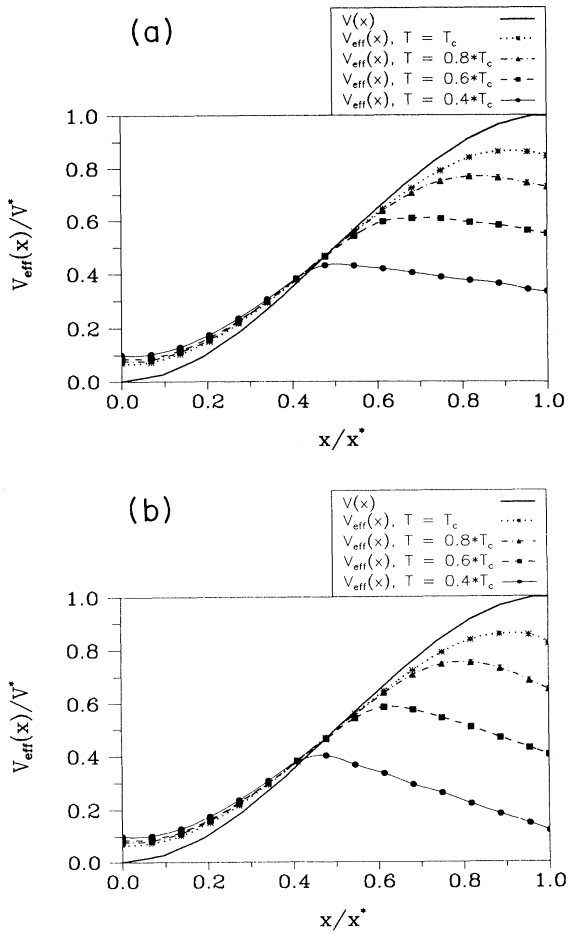

FIG. 5. Effective potential $V_{\text{eff}}(x)$ at different temperatures for the modified cubic parabola potential of Sec. IV with (a) $V_m = -V^*/3$ and (b) $V_m = -V^*$. See the figure for a key to the different curves.

a lower value of $V_m = -V^*$, the centroid approximation fails, yielding a rate constant that unphysically grows as temperature decreases. For temperatures close to T_c the result is almost insensitive to V_m, giving a rate that is in a very good agreement with the exact value.

The effective potential is plotted in Fig. 5 for different temperatures. In accord with semiclassical considerations, the transition state $x^\dagger$ shifts to the left towards the minimum of the potential as T decreases. For temperatures close to T_c the shape of the effective potential near the transition state is insensitive to V_m, while for $T \approx 0.5 T_c$ the effective potential is considerably different for the two different values of V_m, leading to different results for k.

We therefore conclude that the modification of an unstable potential suggested above works only if the modified potential is not too asymmetric or temperature is not too low. For the particular choice of $V_m = -V^*/3$ at low temperatures the result of the centroid method differs from the data of [23] by about 25%, while the accuracy of the instanton method is 10%. The reason why the centroid method may turn out to be less accurate than the semiclassical approximation is discussed in the Appendix.

V. DISCUSSION

We have demonstrated in this paper that the centroid formula conjectured by Gillan [1] can be derived as a stationary phase limit of the imaginary part of the free energy. In order to get the correct answer with the centroid method one should redefine the transition state [2,13] as the point where the centroid density (8) is minimal. For an asymmetric potential the transition state tends to the minimum of the potential and the effective barrier $V^\dagger_{\rm eff}$ vanishes. However, the transition rate is proportional to $\exp(-\beta V^\dagger_{\rm eff})$ and remains finite. The finiteness of $\beta V^\dagger_{\rm eff}$ justifies use of the steepest-descent approximation Eq. (10) when evaluating the imaginary part of the free energy.

As shown by recent studies [2,30], for a symmetric or nearly symmetric barrier the centroid approximation yields an accurate result and is seemingly superior to semiclassical methods if the barrier is not too high or is highly anharmonic. (More quantitatively, the semiclassical approximation is accurate if the size of quantum fluctuations around the stationary bounce solution [16,17] is small compared to the length at which anharmonic corrections to the potential come into play.)

We have tested the centroid method for an asymmetric potential and found that if the asymmetry is not too large or temperature not too low, the centroid method yields a reasonable estimate for the rate below the crossover temperature. The accuracy of the method deteriorates as temperature is decreased, being practically exact at $T \approx T_c$. For temperatures close to zero the result of the centroid method turns out to be less accurate than that of semiclassical periodic orbit theory. This conclusion appears surprising at first sight since the centroid method, involving "fewer stationary phase integrations" (in fact, only one), seems to be "less approximate" than the pure stationary phase approximation to the free-energy path integral exploited by the semiclassical method. The explanation lies in the analytical continuation procedure that inherently involves the stationary phase approximation. For a strongly asymmetric potential the direction of the x_0 coordinate in the space of Fourier components of the thermal path is considerably different from the direction of the unstable normal mode at the saddle point of the action, thereby leading to an incorrect value of imaginary part of the analytically continued free energy.

It follows from the discussion of Secs. II and III that quantum TST can be formulated in much the same way as classical TST: The quantum theory deals with saddle points of the action in the (infinite-dimensional) space of thermal paths, while the classical theory is formulated in terms of the saddle points of the potential in the configuration space. Loosely speaking, as the temperature is raised above T_c, all relevant thermal paths collapse to points in the configuration space such that the quantum averaged potential of Eq. (8) becomes the classical effective potential Eq. (33). From this perspective, the best choice of the "reaction coordinate" in the space of thermal paths should be the one suggested by the above analogy, the minimum action path that passes through the saddle point of the action and coincides with the normal mode at this point. To determine the effective potential, thermal paths should be constrained in the hyperplane perpendicular to the MAP. This prescription avoids the divergencies that arise when the centroid constraint is used and therefore it should produce meaningful results at arbitrarily low temperatures without invoking additional tricks. We intend to examine the feasibility of such an approach in our future work.

For clarity, our discussion in this paper focused on one-dimensional potentials. A multidimensional generalization of the theory is provided by Eq. (18). In the dissipative tunneling model [31] the system coordinate x is coupled linearly to the bath of harmonic oscillators; the bath degrees of freedom can be integrated out, leading to quadratic nonlocal terms in the action of the particle. Adding such a quadratic term does not change any of our conclusions and, moreover, does not complicate numerical evaluation of the centroid density using Monte Carlo path-integral techniques.

As a final remark, we note that recently the idea of *electronic* centroid has been used to study electronically nonadiabatic chemical reactions [29,30,32,33], that is, those that involve transitions between two distinct potential-energy surfaces. Egger, Mak, and Weiss [33] showed strong correlation between the nuclear and the electronic centroids. The treatment in those papers was based on perturbation theory in electronic coupling, assuming electronically nonadiabatic transitions.

On the other hand, it has been shown [16,17,34] that the problem of nonadiabatic tunneling can be formulated semiclassically in terms of *nuclear* bounce trajectories, interpolating smoothly from the electronically nonadiabatic to the adiabatic tunneling regime. Can a general transition-state-like theory be formulated in this case? We believe that the answer is yes: Different electronic states can be described as corresponding to the eigenval-

ues of the Pauli matrix σ_z. In electronic centroid theories [29,30,32–34] σ_z plays the role of the reaction coordinate and the centroid of a thermal path is given by $\sigma_c=\beta^{-1}\int_0^\beta d\tau\,\sigma_z(\tau)$. Therefore σ_z may be treated as an additional degree of freedom and incorporated into the multidimensional centroid theory outlined in Sec. II.

ACKNOWLEDGMENTS

D.E.M. is grateful to Hannes Jonsson, Gregory Mills, and Gregory K. Schenter for stimulating discussions and correspondence. We thank Nancy Makri for useful comments.

APPENDIX: A SIMPLE TOY MODEL

A toy model presented below illustrates the failure of the centroid method for strongly asymmetric potentials. The model is based on representing the action Eq. (6) in terms of the Fourier components $x_0,x_1,\ldots$ of the path $x(\tau)$,

$$\int_0^\beta d\tau\,H(x,\dot{x})=S(x_0,x_1,\ldots)\ .$$

The centroid constraint amounts to setting $x_0=x_c$. In the Fourier component space any path $x(\tau)$ is represented by a point. For example, saddle points of the surface $S(x_0,x_1,\ldots)$ represent bouncelike trajectories, while the points $x_1=x_2=\cdots=0$ correspond to static solutions $x(\tau)\equiv x_0$.

For the potential of Eq. (36) the action is a polynomial that contains quadratic and cubic terms in x_n. In order to somehow mimic the properties of such a function, consider a two-dimensional polynomial of the form

$$S(x_0,x_1)=0.5x_0^2(1-x_0)+0.65x_1^2-x_1^2x_0-0.5x_1^3\ . \tag{A1}$$

We found that this function very closely reproduces the properties of the action for a cubic parabola potential. The choice of the coefficients of the cubic polynomial of Eq. (A1) is rather arbitrary and is only dictated by convenience. The contour map of this function is shown in Fig. 6. The function has one minimum $x_1=x_0=0$ and one saddle point $x_1=x_1^*$, $x_0=x_0^*$. The partition function is defined as

$$Z=\int dx_0dx_1\exp[-\beta S(x_0,x_1)]\ . \tag{A2}$$

This integral diverges and is to be regularized by extending the integration into a complex plane. One way of doing that is to use the steepest-descent approximation near the saddle point, which gives the dominant contribution to the imaginary part of Z.

Introducing the unstable (s) and stable (t) normal modes at the saddle point, the action can be represented as

$$S(s,t)=S(x_0^*,x_1^*)+\tfrac{1}{2}\omega_t^2t^2-\tfrac{1}{2}\omega_s^2s^2\ . \tag{A3}$$

Expressing Eq. (A2) in terms of the new coordinates, the source of divergence is integration over s. Continuing the integration over s into the complex plane, the imaginary part of Z is equal to

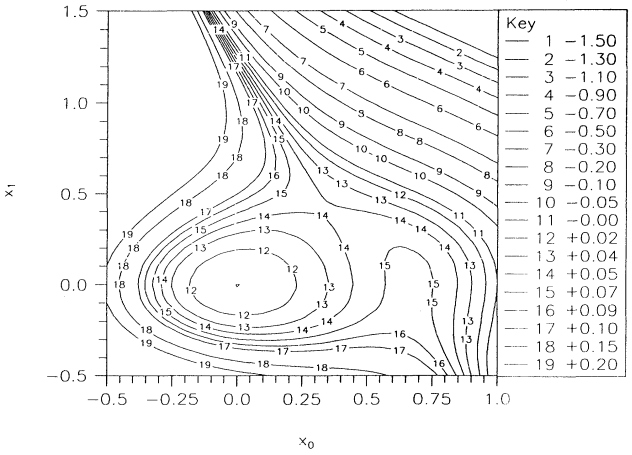

FIG. 6. Contour map for the function $S(x_0,x_1)$ given by Eq. (A1).

$$\mathrm{Im}Z=\frac{\pi}{\beta\omega_t\omega_s}\exp[-\beta S(x_0^*,x_1^*)]\ . \tag{A4}$$

This is nothing but the bounce or instanton approximation for the action of Eq. (A1).

Next, let us examine the possibility of analytical continuation offered by the effective potential idea: After integrating over x_1 one is left with the centroid density $\rho(x_0)$ that is to be integrated over x_0. However, it is easy to see that for every fixed x_0 the integrand is an exponential of a cubic polynomial and therefore the integral over x_1 diverges. For fixed $x_0<x_0^*$ the action $S(x_0,x_1)$ has a minimum and a maximum; ignoring the divergence of the integral and taking into account only the contribution from these local minima, one immediately arrives at the semiclassical effective potential. As discussed in Sec. III–V, this potential corresponds to local minima of the centroid-constrained action, which lie on the steepest-descent line that connects the action minimum and the saddle point (MAP). The stationary points that correspond to the maxima of S for every given x_0 can also be found numerically in the cubic parabola model Eq. (36); they are identified as bouncelike solutions that have action greater than βV^*, thus supporting our conjecture that the two-dimensional model of Eq. (A1) reproduces correctly the topology of the action in the Fourier space. We therefore find that the centroid coordinate x_0 is not the right choice of the unstable mode because the integral over x_1 is still divergent.

From this model it can also be understood why the modification of the potential proposed in Sec. IV did not completely cure the problem. If the action S is bounded from below by some finite value $S_{\min}$, then the centroid density $\int dx_1\exp[-\beta S(x_0,x_1)]$ will be dominated either by the value of $\exp[-\beta S(x_0,x_1)]$ at the point where the action reaches its local minimum, as in the semiclassical approximation for the effective potential or by approxi-

mately $\exp(-\beta S_{\min})$, whichever is greater. In the latter case, by increasing the asymmetry of the potential, the value of $\exp(-\beta S_{\min})$ and consequently the value of the rate constant one obtains from the centroid approximation can be made arbitrarily large, which is apparently incorrect. Only if the contributions from the points that are far from the saddle point are disregarded can one obtain the correct value of the rate constant. That is why, paradoxically enough, use of the semiclassical approximation to the effective potential, which, as we have seen before, is incorrect for the cubic parabola potential of Sec. IV, yields the correct semiclassical limit of the rate constant, while the true effective potential leads to an infinite rate.

[1] M. J. Gillan, J. Phys. C **20**, 3621 (1987).

[2] G. A. Voth, D. Chandler, and W. H. Miller, J. Chem. Phys. **91**, 7749 (1989).

[3] G. A. Voth, Chem. Phys. Lett. **170**, 289 (1990); G. A. Voth and E. V. O'Gorman, J. Chem. Phys. **94**, 7342 (1991); D. Li and G. A. Voth, J. Phys. Chem. **95**, 10425 (1991); J. Lobaugh and G. A. Voth, Chem. Phys. Lett. **198**, 311 (1992); J. Chem. Phys. **97**, 4205 (1992); Y. C. Sun and G. A. Voth *ibid.*, **98**, 7451 (1993); J. Lobaugh and G. A. Voth, *ibid.*, **100**, 3039 (1994).

[4] R. P. McRae, G. K. Schenter, B. C. Garrett, G. R. Haynes, G. A. Voth, and G. C. Schatz, J. Chem. Phys. **97**, 7392 (1992).

[5] G. K. Schenter, M. Messina, and B. C. Garrett, J. Chem. Phys. **98**, 8525 (1993); **99**, 1674 (1993); **99**, 8644 (1993).

[6] J.-K. Hwang and A. Warshel, J. Phys. Chem. **97**, 10053 (1993).

[7] G. Mills and H. Jonsson, Phys. Rev. Lett. **72**, 1124 (1994).

[8] G. A. Voth, J. Phys. Chem. **97**, 8365 (1993).

[9] M. Gillan, Phys. Rev. Lett. **58**, 563 (1987); Philos. Mag. A **58**, 257 (1988).

[10] G. K. Schenter, G. Mills, and H. Jonsson, J. Chem. Phys. **101**, 8964 (1994).

[11] G. Mills, H. Jonsson, and G. K. Schenter, Surf. Sci. **324**, 305 (1995).

[12] R. P. Feynman and A. R. Hibbs, *Quantum Mechanics and Path Integrals* (McGraw-Hill, New York, 1965).

[13] A. A. Stuchebrukhov, J. Chem. Phys. **95**, 4258 (1991).

[14] M. Topaler and N. Makri, J. Chem. Phys. **101**, 7500 (1994).

[15] W. H. Miller, J. Chem. Phys. **62**, 1899 (1975); S. Chapman, B. C. Garrett, and W. H. Miller, *ibid.*, **63**, 2710 (1975).

[16] V. A. Benderskii, V. I. Goldanskii, and D. E. Makarov, Phys. Rep. **233**, 195 (1993).

[17] V. A. Benderskii, D. E. Makarov, and C.A. Wight, *Chemical Dynamics at Low Temperatures* (Wiley, New York, 1994).

[18] V. A. Benderskii, S. Yu. Grebenshchikov, E. V. Vetoshkin, G. V. Milnikov, and D. E. Makarov, J. Phys. Chem. **98**, 330 (1994).

[19] R. P. Feynman and H. Kleinert, Phys. Rev. A **34**, 5080 (1986).

[20] P. Hänggi, P. Talkner, and M. Borkovec, Rev. Mod. Phys. **62**, 251 (1990).

[21] N. Moiseev and J. O. Hirschfelder, J. Chem. Phys **88**, 1061 (1988).

[22] U. Weiss, H. Grabert, P. Hänggi, and P. Riseborough, Phys. Rev. B **35**, 8535 (1987).

[23] W. Hontscha, P. Hänggi, and E. Pollak, Phys. Rev. B **41**, 2210 (1990).

[24] C. G. Callan and S. Coleman, Phys. Rev. D **16**, 1762 (1977).

[25] Alternatively, the rate can be evaluated semiclassically from the flux across the dividing plane by using the traditional WKB theory; see Ref. [15]. The equivalence of this approach and the instanton theory has been demonstrated by P. Hänggi and W. Hontscha, J. Chem. Phys. **88**, 4094 (1988); Ber. Bunsenges; Phys. Chem. **95**, 379 (1991).

[26] I. Affleck, Phys. Rev. Lett. **46**, 388 (1981).

[27] J. D. Doll, J. Chem. Phys. **81**, 3536 (1984).

[28] H. Kleinert, Chem. Phys. Lett. **137**, 162 (1986).

[29] J. N. Gehlen and D. Chandler, J. Chem. Phys. **97**, 4958 (1992).

[30] C. H. Mak and J. Gehlen, Chem. Phys. Lett. **206**, 130 (1993).

[31] A. O. Caldeira and A. J. Leggett, Ann. Phys. (N.Y.) **149**, 374 (1983).

[32] P. G. Wolynes, J. Chem. Phys. **87**, 6559 (1987).

[33] R. Egger, C. H. Mak, and U. Weiss, J. Chem. Phys. **100**, 2651 (1994).

[34] P. G. Wolynes, J. Chem. Phys. **86**, 1957 (1987).